### — ATOMS, MOLECULES, OPTICS —

# ON THE INFLUENCE OF ELECTRON BEAM CHARACTERISTICS ON HARMONIC RADIATION IN SINGLE-PASS FREE-ELECTRON LASERS

© 2024 K. V. Zhukovsky

Lomonosov Moscow State University, Faculty of Physics, Moscow, 119991 Russia e-mail: zhukovsk@physics.msu.ru

Received May 25, 2023 Revised April 14, 2024

Accepted April 14, 2024

Abstract. Currently, coherent radiation of free-electron lasers (FEL) is increasingly being used in many fields of science and technology. In applied and theoretical research, an important effect is the nonlinear second harmonic generation in materials and on surfaces as a response to irradiation. FELs are used as light sources that generate coherent radiation in the range from visible to X-ray. However, the second harmonic of the FEL itself is undesirable as it masks the studied response at the same frequency. We analytically investigate the influence of electron beam parameters on FEL radiation; study the generation of harmonics, especially the second; analyze the main factors causing the appearance of the second harmonic in the FEL spectrum. The influence of beam parameters is examined: cross-section, emittance, Twiss parameters, and energy spread, both separately and together, on the gain length and FEL harmonic generation using the well-documented LEUTL FEL as an example. The effect of these parameters on the radiation power of harmonics, especially the second, is analyzed. The influence of the undulator field harmonic on FEL harmonic radiation is also investigated. It is proposed to increase the electron energy spread twofold to the maximum possible value that ensures electron bunching while simultaneously reducing the second harmonic content in the FEL spectrum by one to two orders of magnitude. It is also suggested to use a weak undulator field harmonic for the same purpose — to suppress the FEL harmonic.

### **DOI:** 10.31857/S004445102411e026

### 1. INTRODUCTION

Undulator radiation (UR) is the radiation of relativistic electrons in a spatially periodic magnetic field. It was predicted by Ginzburg [1] in the mid-20th century and shortly thereafter obtained by Motz [2]. UR from electron bunches is incoherent when the bunch length is significantly larger than the wavelength; this occurs in most cases, but not always. Coherent UR from electrons in bunches whose length is comparable to or smaller than the wavelength was also predicted by Ginzburg and obtained by Madey [3] in a free electron laser (FEL) in the millimeter range. In the 21st century, with the emergence of new technical capabilities and highquality beams. FELs have advanced into the X-ray range and are actively used as radiation sources in many fields. FELs represent fourth-generation radiation sources and are a logical development of synchrotron radiation (SR) sources in the 20th century [4–7]; FEL theory and practical applications

are presented in extensive literature (see, for example, [8–14]). Without dwelling on details, we can say that coherent radiation in FEL undulators occurs from electron microbunches spaced apart by the radiation wavelength, and the microbunches themselves are smaller than the radiation wavelength [1]. The main instruments in a modern FEL are the accelerator and undulator; the first accelerates electrons to high energy while maintaining low energy spread and emittance, the second represents the generation and radiation system in the FEL. Electron grouping into microbunches occurs under the action of the Lorentz force of the electromagnetic radiation wave in the undulator; it accelerates electrons located behind the wave nodes of UR and decelerates electrons located ahead of the wave nodes of UR. Electrons in the undulator group not only at the radiation wavelength; grouping also occurs at harmonic wavelengths, but weaker than at the fundamental wavelength. The most common type of undulator is planar. On the

axis of a planar undulator, radiation from adjacent periods arrives in phase for odd harmonics and in antiphase for even ones. Thus, in a planar undulator, ideally only odd harmonics are radiated on the axis, while even ones are suppressed. In reality, the electron beam has a finite cross-section, and both odd and even harmonics are radiated on the axis. In undulators with a double-periodic field, a weak harmonic of the main undulator field allows, within certain limits, to regulate the radiation of UR harmonics. Additionally, in real undulators, a field harmonic is always present, if only because an ideal monoharmonic field throughout the undulator gap does not satisfy Maxwell's equations.

FEL radiation harmonics can be useful when higher frequency radiation is required from electrons of a given energy. However, the presence of harmonics does not always play a positive role. For example, the second FEL harmonic masks and complicates the study of the nonlinear second harmonic generation (SHG) response [15] of the medium when studying material properties [16–18], films and surfaces [19] in physics [20] and chemistry [21], organic compounds [22, 23] and others. In the XUV range [24], even harmonics generation was observed during irradiation TiM<sub>2,3</sub>, in the visible range [25, 26] nonlinear generation of even harmonics of the fundamental tone occurs when studying physicochemical properties of molecules, films and surfaces and may indicate a violation of internal symmetry of the studied samples [21, 23]; nonlinear response in the X-ray range is used in studies using nuclear resonance. Since the power of the SHG response is naturally significantly lower than the source power, the second harmonic content of the FEL should be minimal.

FEL harmonic powers can be calculated analytically using the Bessel coefficient formalism taking into account all major factors in generalized Bessel functions: undulator parameters, beam parameters and its deviation from the axis, emittance, focusing, etc. Analytical expressions for various undulators taking into account field harmonics are given in many works (see, for example, [27–33]). Using these, one can calculate the spontaneous radiation power taking into account major losses, but in FEL it is impossible to calculate exactly the evolution of harmonic power along the undulator length due to the complexity of the equations system for charges and fields and the enormous

number of electrons. Calculation in FEL models is performed numerically using special programs (see, for example, [34–36] and others). The results of numerical solution of electron motion and radiation equations in the undulator magnetic field, taking into account field harmonics and interaction with the SR wave field, agree with experimental power values measured along the undulator length within an order of magnitude for fundamental tone power; for harmonics, the spread of values is larger [37–41]. The disadvantage of numerical models is that they do not allow to isolate and analyze separately the influence of factors on FEL harmonic generation.

We use an approximate analytical description of the exponential growth of harmonic power in FEL, which includes precisely calculated Bessel coefficients. The latter determine the Pierce parameters of harmonics, their generation, and make it possible to identify the role of various factors in harmonic radiation. Using analytical expressions, we investigate the influence of undulator and beam parameters on FEL radiation to possibly reduce the radiation power of the second harmonic while maintaining the power of the fundamental tone. Below, we examine the influence of the beam cross-section, emittance, and energy spread on FEL radiation.

### 2. APPROXIMATE ANALYTICAL DESCRIPTION OF FEL HARMONIC POWER

The basic power formulas for calculating FEL harmonic radiation have been published repeatedly before, for example, in [27–33]; the results are consistent with numerical models [34, 35, 42–45] and data from all major FELs worldwide in the range from visible to hard X-ray [37–41]. Below we will present only the basic expressions for FEL harmonic power at saturation. The harmonic n SR at an effective angle  $\Theta$  to the undulator axis has the following wavelength:

$$\lambda_n = \frac{\lambda_u}{2n\gamma^2} \left[ 1 + \frac{k^2}{2} + (\gamma \Theta)^2 \right],\tag{1}$$

where

$$k = H_0 \lambda_u e / 2\pi m c^2 \approx 0.9337 H_0 [T] \lambda_u [cm]$$

• is the undulator parameter, e is the electron charge,  $\lambda_u$  is the undulator period,  $H_0$  is its field amplitude. For a planar undulator, the Bessel coefficients of  $f_{n:x,y}$  x- and y-polarizations of the

570 ZHUKOVSKY

*n*-th harmonic, considering its betatron splitting, have the form [46]

$$f_{n,x} \approx \sum_{p} \tilde{J}_{p} \left| \left( J_{n+1}^{n} + J_{n-1}^{n} \right) + J_{n}^{n} \frac{2}{k} \gamma \theta \cos \varphi \right|,$$

$$f_{n,y} \approx \sum_{p} \left( \tilde{J}_{p} \left| J_{n}^{n} \frac{2}{k} \gamma \theta \sin \varphi \right| + + + J_{n}^{n} \frac{\sqrt{2} \pi y_{0}}{\lambda_{u}} \left( \tilde{J}_{p+1} - \tilde{J}_{p-1} \right) \right|,$$

$$(2)$$

where  $y_0$  is the electron beam cross-section, p is the betatron harmonic in the spectrum line n,  $\varphi$  is the polar angle,  $\theta$  is the azimuthal angle from the axis,  $J_n^m$  and  $\tilde{J}_p$  are generalized Bessel-type functions:

$$J_n^m = \int_{-\pi}^{\pi} \frac{d\alpha}{2\pi} \times \left\{ i \left[ n\alpha + \frac{mk^2 \left( \frac{\sin(2\alpha)}{4} + \frac{2}{k} \gamma \theta \cos \varphi \sin \alpha \right)}{1 + \gamma^2 \theta^2 + (k^2/2)} \right] \right\}, (3)$$

$$\tilde{J}_p = \int_{-\pi}^{\pi} \frac{d\alpha}{2\pi} \times \left\{ i \left[ p\alpha - \frac{4\pi \theta y_0 \gamma^2 \sin \alpha}{\lambda_u (1 + k^2/2)} - \frac{\pi^2 \gamma y_0^2 k \sin(2\alpha)}{\sqrt{2} \lambda_u^2 (1 + k^2/2)} \right] \right\}.$$

The Bessel coefficients (2) and the generalized Bessel functions (3) included in them determine harmonic generation and depend on beam and undulator parameters in a complex way, both explicitly and implicitly. The undulator parameter k

together with the angle  $\theta$  enters the factor  $\sim \frac{2}{k} \gamma \theta$  for the even harmonics Bessel function  $J_n^n$ ; the beam cross-section enters as a factor  $y_0$  in the betatron contribution of even harmonics

$$f_{n;y} \propto \sum_{p} J_{n}^{n} \frac{\sqrt{2} \pi y_{0}}{\lambda_{u}} (\tilde{J}_{p+1} - \tilde{J}_{p-1});$$

the angular contribution  $\sim \frac{2}{k} \gamma \theta$  is also present in

the Bessel function argument  $J_n^m$ , and the beam cross-section enters the arguments of betatron Bessel functions  $\tilde{J}_p$  both independently and jointly with the angle dependence  $\theta$ . Considering the electron-photon interaction angle  $\bar{\theta} \approx \sigma_{x,y}/L_g$  we estimated

that for all major FELs with beam cross-sections of  $\sigma_{x,y} \approx 25 - 250 \, \mu m$ , the argument

$$\frac{4\pi\theta y_0 \gamma^2}{\lambda_u (1 + k^2/2)}$$

is an order of magnitude larger than the argument

$$\frac{\pi^2 \gamma y_0^2 k}{\sqrt{2} \lambda_u^2 (1 + k^2/2)}.$$

Thus, the Bessel coefficients  $f_n$  have a complex dependence on many undulator and beam parameters. Below we will analyze their influence on the LEUTL FEL radiation.

It is important that in the Bessel coefficients for FEL, the effective angle  $\overline{\theta} \approx \sigma_{x,y}/L_g$  should be taken into account in the angular dependence, at which electrons on average "see" the radiation at the FEL gain length and interact with it [27, 46]. The angular contribution from  $\bar{\theta}$  is determining, as this angle is usually significantly larger than the divergence angle. This is different from the Bessel coefficients for spontaneous UR, where the beam divergence  $\theta_{x,y}$  and the angle between the observer's direction and the undulator axis are determining. Thus, in the Bessel coefficients for FEL, the beam cross-section  $\sigma_{x,v}$  plays a role not only in betatron contributions, which have the order of  $1/\gamma$  and are small in the relativistic case, but also in angular contributions that determine the generation of even FEL harmonics. In a long undulator of X-ray FELs, beam deviation from the axis comparable to the beam cross-section is also possible (see, for example, [37]). Let us emphasize the dependence of values not on the emittance  $\varepsilon_{x,y}$ , but on the cross-section

$$\begin{split} \sigma_{x,y} &= \sqrt{\epsilon_{x,y} \beta_{x,y}} \,, \\ \beta_{x,y} &= \epsilon_{x,y} \, / \, \theta_{x,y}^2 = \sigma_{x,y}^2 \, / \epsilon_{x,y} \end{split}$$

• Twiss parameter, and on the angle  $\theta$ , which includes  $\overline{\theta}$ ; beam emittance

$$\varepsilon_{x,y} = \sigma_{x,y} \theta_{x,y}$$

is secondary in this context. Betatron oscillations in a finite cross-section beam lead to the splitting of the harmonic radiation spectrum line n into betatron harmonics p, which are separated by a frequency much lower than the radiation frequency,

$$\omega_{\beta} \approx \frac{\omega_n k}{\sqrt{2}n\gamma} \ll \omega_n$$

see [47], at  $\gamma \gg 1$ .

In the theory of stimulated emission, the dimensionless Pierce parameter plays an important role. It is introduced during the process of converting electron motion equations and wave amplification to dimensionless form in such a way that the longitudinal coordinate is normalized to the wave number of the emitted wave  $k = \omega/c$ . In the linear approximation, the wave is amplified according to the following law:  $A(z) \propto \exp(Ckz)$ , where C is the Pierce parameter. Initially, the Pierce parameter C was introduced for Cherenkov-type radiation and klystron-type devices and only later for FEL and cyclotron masers [48]. In FEL theory, the longitudinal coordinate along the device axis is normalized to the undulator wave number  $k_u = 2\pi/\lambda_u$ . Accordingly, in the linear approximation, the wave is amplified according to the law

$$A(z) \propto \exp(\rho k_{\mu} z)$$
,

where  $\rho$  is the Pierce parameter in FEL, which is sometimes called the FEL-parameter in English-language articles. The Pierce parameter  $\rho$  in FEL differs from the Pierce parameter C in normalization. For example, the FEL Pierce parameter  $\rho$  determines the gain length:

$$L_{n,g} \approx \frac{\lambda_u}{4\pi\sqrt{3}\,n^{1/3}\rho_n},\tag{4}$$

and the FEL electron efficiency in saturation mode simply coincides with  $\rho$  within a factor of square root of two [8–11], so that the maximum (though not necessarily achievable) power of the n-th harmonic is written as follows:

$$P_{F,n} \approx \sqrt{2} \, \rho_n P_{beam}$$

where  $P_{beam} = EI_0$  is the electron beam power. There is a difference from the Pierce parameter C, in terms of which scientists define the device efficiency as  $C\gamma^2$ , where  $\gamma$  is the relativistic mass factor of the electron. The Pierce parameter  $\rho$  for FEL is written as follows (see [8–14]):

$$\rho_n = \frac{1}{2\gamma} \left( \frac{J}{4\pi i} \right)^{1/3} (\lambda_u k |f_n|)^{2/3}, \tag{5}$$

where  $f_n$  is the Bessel coefficient (2) of the *n*-th harmonic,  $J = I_0/\Sigma$  is the current density,  $I_0$  is the electron current in a beam of cross-section  $\Sigma = 2\pi\sigma_x\sigma_y$ ,  $i[A] = 4\pi\epsilon_0mc^3/e \approx 1.7045\cdot 10^4$  is the Alfven current constant. Losses due to finite beam

cross-section, emittance, and energy spread increase the gain length  $L_g$  and decrease the harmonic power  $P_{n,F}$ , which, moreover, is not always achievable due to saturation of the entire FEL, which usually occurs before harmonic saturation. The gain length correction (and consequently, power correction) is best described by Ming Xie's formula [49, 50]:

$$L_g = L_{g0}(1 + \Lambda),$$

where  $\Lambda$  is a polynomial of fractional degree with nineteen coefficients. G. Dattoli's formulas [51, 52] for correction of the Pierce parameter, gain length, and power agree well with this:

$$\rho_n \to \frac{\rho_n}{\kappa}, \quad \kappa = \sqrt[3]{1 + \frac{\lambda_u \lambda_n}{16 \pi \rho_n \Sigma}},$$
 (6)

$$L_{n,g} \to L_{n,g} \kappa \Phi_n,$$
 (7)

$$L_s \approx 1.07 L_g \ln \frac{9 \eta_1 P_F}{P_0}, \tag{8}$$

$$P_{n,F} \approx \sqrt{2} \frac{\eta_1}{\kappa^2} \rho_n P_{beam}. \tag{9}$$

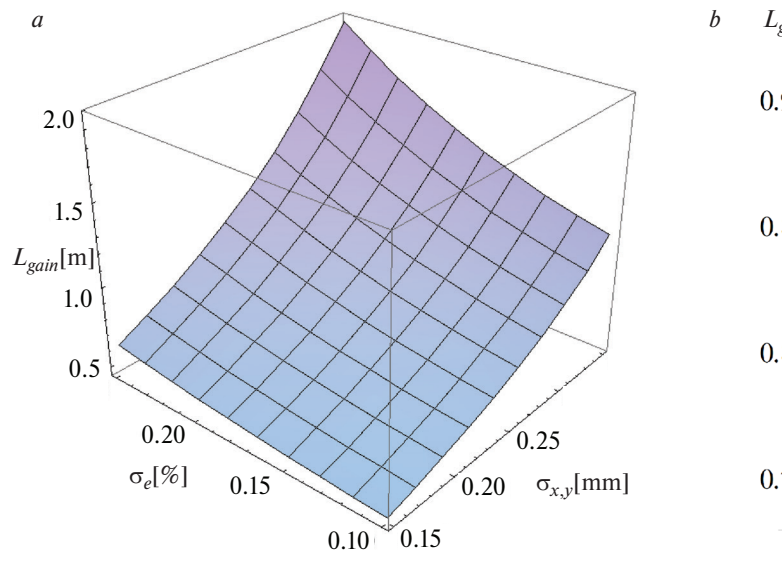
The high sensitivity of electron-photon interaction at harmonic wavelengths n to electron energy spread and other losses is taken into account phenomenologically. Thus, in (6) the energy spread  $\sigma_{\varepsilon}$  and emittance  $\varepsilon_{x,y}$  are accounted for by coefficients  $\Phi$  and  $\eta$ , which we previously calibrated using data from all major operating FELs in ranges from visible to X-ray [29–31]:

$$\Phi_n \approx \left(\zeta^{\sqrt{n}} + 0.165\mu_{\varepsilon,n}^2\right) e^{0.034\mu_{\varepsilon,n}^2},$$

$$\mu_{\varepsilon,n} \approx \frac{2\sigma_e}{n^{1/3}\tilde{\rho}_n},$$
(10)

$$\eta_n \approx 0.942 \left[ e^{-\Phi_n(\Phi_n - 0.9)} + \frac{1.57(\Phi_n - 0.9)}{\Phi_n^3} \right]$$

The coefficient  $\zeta$  approximately conveys the dependence on Twiss parameters and emittance and has a complex expression [52]; overall it is close to unity,  $\zeta \approx 1-1.05$ , for most modern facilities with low emittance,  $\gamma \varepsilon \sim 10^{-6} \, \text{m} \cdot \text{rad}$ , and only for beams with large emittance,  $\gamma \varepsilon > 10^{-5} \, \text{m} \cdot \text{rad}$ , we have  $\zeta \approx 1.1-1.4$ , which increases the gain length. The initial power in FEL is given from a seed radiation source or in self-amplified



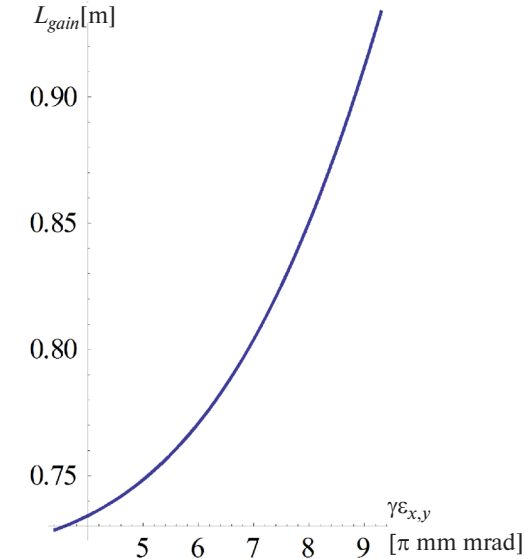


Fig. 1. Dependencies of LEUTL FEL gain length on energy spread  $\sigma_e$  and cross-section  $\sigma_{x,y} = \sigma$  of electron beam with given Twiss parameter  $\beta = 1.5$  m (a) and on beam emittance  $\gamma \varepsilon_{x,y}$  (b) in experiment with cross-section  $\sigma_{x,y} = 0.25$  mm; electron energy spread  $\sigma_e = 0.001$ ; current  $I_0 = 210$  A

spontaneous emission SASE FEL from the coherent component of electron bunch noise:

$$P_{0,n} \approx 1.6 \rho_n^2 e \, 4\pi c \, P_{beam} / I_0 \lambda_n$$

see [53]. Harmonic power is usually limited by saturation of the fundamental tone and the entire FEL, which occurs before harmonic saturation and is accompanied by growth of induced electron energy spread. Therefore, in nonlinear growth mode, the saturation power of the n-th harmonic is usually less than  $P_{F,n}$ ; at the saturation length

$$L_s \approx 1.07 L_g \ln \frac{9 \eta_1 P_{F,1}}{P_{0,1}}$$

the harmonic power estimate is:

$$P_{n,F} \approx \eta_n \frac{P_{1,F}}{\sqrt{n}} \left( \frac{f_n}{nf_1} \right)^2$$

see [51, 52]. It does not take into account the oscillations of power in saturation, as well as the continuing slow increase in harmonic power after the fundamental tone has saturated. These effects are accounted for phenomenologically in the formula we developed based on analysis of harmonic behavior in saturation mode at undulator length  $z \sim L_s$  in the world's main operating FELs:

$$\widehat{P}_{n,F} \approx P_{n,F} \left( \frac{z}{L_s} \right)^{\frac{n}{2}} |_{z \sim L_s} \times$$

$$\times \left[0.77 + 0.23\cos\frac{n(z - L_s)}{1.3L_g}\right] - \frac{\tilde{P}_{n,F}}{2.5},\tag{11}$$

where

$$\tilde{P}_{n,F} = P_{n,F} \mid_{\mu_{\varepsilon,n} \to \tilde{\mu}_{\varepsilon,n}, \tilde{\Phi}_{n}(\tilde{\mu}_{\varepsilon,n}), \eta(\tilde{\mu}_{\varepsilon,n})},$$
(12)
$$\tilde{\mu}_{\varepsilon,n} \approx \frac{2n^{2/3} \sigma_{e}}{\tilde{\rho}_{n}}.$$

The theoretical expression for power (11) takes into account exact Bessel coefficients (2). The result agrees well with known data from all most famous FELs (see [27–33]); moreover, result (11) better conveys experimental data of FEL harmonic power than theoretical estimates in [54, 55], as shown in [30, 56, 57].

## 2.1. Influence of electron beam parameters on FEL gain length

Let us consider the well-documented LEUTL FEL with radiation at wavelength  $\lambda_1 \approx 540$  nm. LEUTL undulator data: period  $\lambda_u = 3.3$  cm, section length  $L_u = 2.4$  m, undulator parameter k = 3.1, FEL beam parameters: current  $I_0 = 210$  A, electron energy E = 217 MeV, energy spread  $\sigma_e = 1 \cdot 10^{-3}$ , average emittance  $\gamma \varepsilon_{x,y} \approx 6.2\pi \cdot 10^{-6}$  mm·mrad, Twiss parameter  $\beta_{x,y} = 1.5$  m, beam cross-section  $\sigma_{x,y} = 0.25$  mm, divergence  $\theta_{div} \approx 0.17$  mrad. We use formulas (2)–(11) to analyze the power of FEL

harmonics and evaluate the possibility of suppressing the second FEL harmonic.

Let us consider the dependence of the FEL gain length calculated by us on various electron beam parameters; the current is considered fixed in all cases. The gain length practically does not depend on the undulator field harmonics. The dependence of gain length on electron energy spread and beam cross-section is constructed using formulas (6), (10) and shown in Fig. 1a at a fixed value of the Twiss parameter  $\beta_{x,y}=1.5$ . The gain length measured in the experiment was  $L_{gain}\approx 0.75$  m, which coincides with our theoretical result for the given installation parameters (see Fig. 1 for  $\sigma_e=0.1\%$ ). The effective angle of electron interaction with radiation in this case is  $\bar{\theta}\approx \sigma_{x,y}/L_{gain}\approx 0.3$  mrad, which gives a value of  $\gamma\bar{\theta}\approx 0.13$ , twice as large as for divergence:  $\theta_{div}\gamma\approx 0.07$ .

When varying the beam cross-section and fixed Twiss parameter  $\beta_{x,y}$ , effective emittance change occurs only through change in cross-section. This case appears important since the cross-section and gain length determine the angle  $\overline{\theta}$ , which, in turn, mainly determines the generation of the second FEL harmonic. Note that the dependence of gain length on electron energy spread  $L_{gain}(\sigma_e)$  at cross-section value  $\sigma_{x,y} = 0.25$  mm practically repeats the dependence on cross-section  $L_{gain}(\sigma_{x,y})$  at energy spread  $\sigma_e = 0.001$ (see Fig. 1a). This appears to be a coincidence, but these parameter values are present in many LEUTL experiments [39, 40]. The dependence  $L_{gain}(\sigma_{x,y})$  at constant current is mainly determined by the change in current density J and the corresponding change in Pierce parameter  $\rho$  (5), as well as the less significant change in parameter  $\kappa$  (6), which describes the influence of emittance on beam diffraction; at the same time, the influence of energy spread  $\sigma_e$  on the gain length is described independently by coefficient  $\mu_{\epsilon}$  (10). With a small electron beam cross-section and correspondingly small emittance, the LEUTL FEL gain length changes little with energy spread variation within wide limits  $\sigma_e \sim 0.1 - 0.3\%$  (see Fig. 1a graph at  $\sigma_{x,y} = 0.1$  mm); at large beam cross-sections,  $\sigma_{x,y} \approx 0.25$  mm, the FEL gain length increases with increasing energy spread. At even larger cross-sections  $\sigma_{x,y} \gg 0.3$  mm and given value  $\beta_{x,y} = 1.5$  m, both the gain length and its dependence on energy spread increase significantly (see Fig. 1a at  $\sigma_{x,y} = 0.4$  mm).

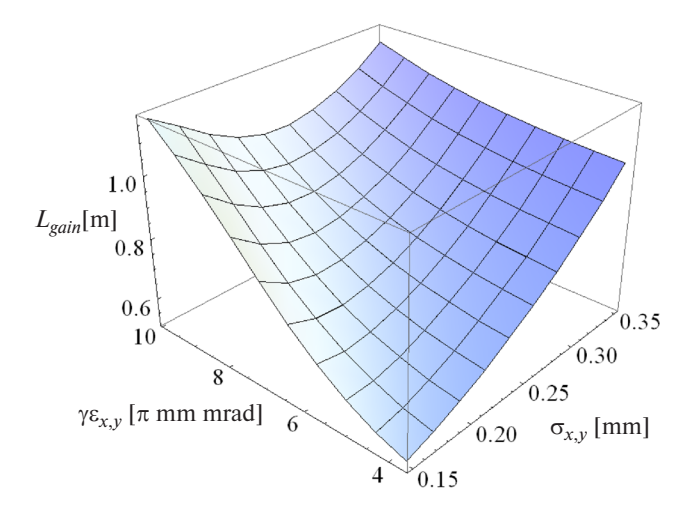


**Fig. 2.** Dependence of LEUTL FEL gain length on emittance and beam cross-section with energy spread  $\sigma_e = 0.001$ ; current  $I_0 = 210 \text{ A}$ 

Let's now consider the possible influence of beam emittance variation  $\varepsilon_{x,y}$  assuming a fixed cross-section  $\sigma_{x,y}$ . In this case, the change in emittance is inversely proportional to the change in the Twiss parameter  $\beta_{x,y}$ , so that

$$\sigma_{x,y} = \sqrt{\varepsilon_{x,y}\beta_{x,y}} = \text{const.}$$

This does not change the current density, parameter  $\kappa$  (6), describing diffraction, and Pierce parameter (5), which determines the gain length and FEL power. We found that the variation of beam emittance at fixed cross-section (see Fig. 1*b*) changes the gain length somewhat less compared to how the variation of cross-section at a given Twiss parameter changes the gain length (compare with Fig. 1*a*).

Expressing the Twiss parameter as  $\beta_{x,y} = \sigma_{x,y}^2 / \epsilon_{x,y}$ , one can fix the emittance  $\epsilon_{x,y}$  and analyze in this case the influence of beam cross-section  $\sigma_{x,y}$  on the gain length. The result is presented in Fig. 2. It differs noticeably from the graphs in Fig. 1.

In the LEUTL FEL, emittance values varied and in different experiments were  $\gamma \epsilon_{x,y} \approx 5.5 - 9 \cdot 10^{-6} \, \text{mm} \cdot \text{mrad}$ . Fig. 2 shows approximately this range of variation and demonstrates how the gain length dependence on cross-section qualitatively changes with emittance variation. At large cross-sections, there is almost no dependence on emittance, while at small cross-sections, the gain length dependence on emittance is strong. Fig. 2 shows that small emittance and small cross-section allow reducing the gain length to approximately 0.6 m, while with large emittance, the cross-section



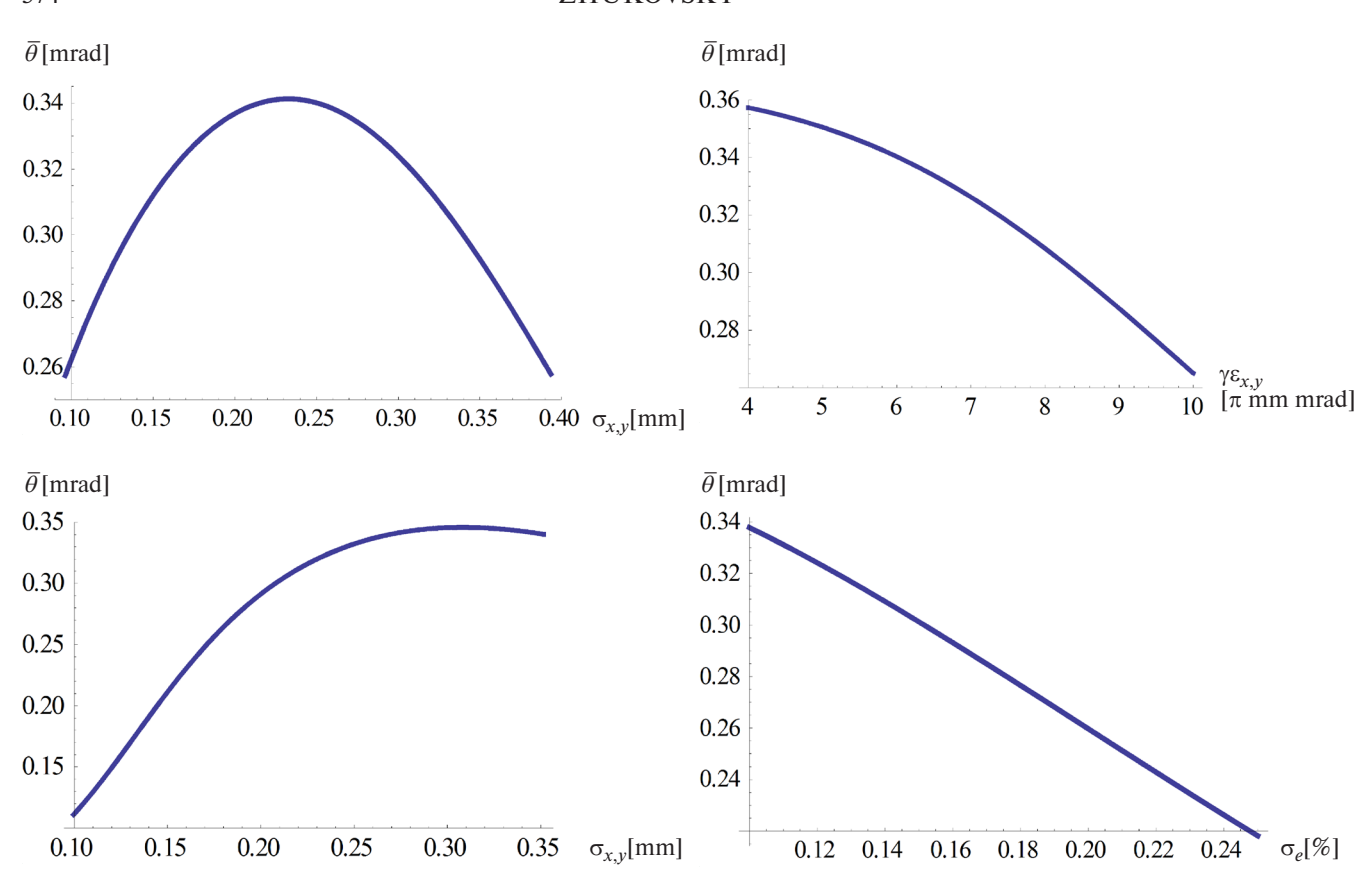


Fig. 3. Dependencies of the electron-photon interaction angle in LEUTL FEL on beam crosssection at given experimental Twiss parameter  $\beta=1.5$  m and energy spread  $\sigma_e=0.001$  (a); on emittance at given experimental cross-section  $\sigma_{x,y}=0.26$  mm and energy spread  $\sigma_e=0.001$  (b); on cross-section at given experimental emittance  $\gamma \varepsilon_{x,y}=6.2\pi \cdot 10^{-6}$  mm-mrad and energy spread  $\sigma_e=0.001$  (c); on energy spread at given  $\gamma \varepsilon_{x,y}=6.2\pi \cdot 10^{-6}$  mm·mrad,  $\sigma_{x,y}=0.26$  mm (d);  $\beta=1.5$  m; energy  $I_0=210$  A

varies in a small interval of 1-1.2 m and shows a minimum at cross-section value  $\sigma_{x,y} = 0.25$  mm, which corresponds to experimental parameters of LEUTL FEL [39, 40]. Naturally, from a practical point of view, it is necessary to reduce the gain length as much as possible to decrease the size and cost of FEL. A shorter gain length is also accompanied by higher FEL power, which is valuable.

We studied the influence of emittance, cross-section, and electron beam energy spread on the effective angle of electron-photon interaction in FEL:  $\bar{\theta} \approx \sigma_{x,y}/L_{gain}$ . Note that changes in beam parameters lead to changes in FEL gain length, as shown in Fig. 1; this affects the angle  $\bar{\theta} \approx \sigma_{x,y}/L_{gain}$ ; furthermore,  $\bar{\theta}$  is directly affected by the beam cross-section itself. The obtained analytical dependence  $\bar{\theta}(\sigma_{x,y}, \, \epsilon_{x,y})$  on beam cross-section and emittance in LEUTL is shown in Figs. 3a,b,c. When changing the beam cross-section due to emittance variation and the experimentally set Twiss parameter  $\beta = 1.5$  m, angle  $\bar{\theta}$  changes within

small limits, as shown in Fig. 3a. Interestingly, the dependence  $\bar{\theta}(\sigma_{x,y})$  has a maximum (see Fig. 3a) and this maximum corresponds approximately to the measured experimental values of LEUTL: cross-section  $\sigma_{x,y}=0.26$  mm and emittance  $\gamma \epsilon_{x,y}=6.2\pi\cdot 10^{-6}$  mm·mrad with energy spread  $\sigma_e=0.001$ . When changing the emittance with a fixed beam cross-section in the experiment, the angle  $\bar{\theta}$  monotonically decreases with increase emittance (see Fig. 3b). Thus, the dependence on emittance in Fig. 3b is quite different from the dependence on the beam cross section in Fig. 3a.

Furthermore, we studied the analytical dependence  $\overline{\theta}(\sigma_{x,y})$  on beam cross-section at experimentally measured emittance  $\gamma \varepsilon_{x,y} = 6.2\pi \cdot 10^{-6} \, \text{mm} \cdot \text{mrad}$ , shown in Fig. 3c. For given emittance  $\gamma \varepsilon_{x,y} = 6.2\pi \cdot 10^{-6} \, \text{mm} \cdot \text{mrad}$ , small cross-sections below experimental give small angles  $\overline{\theta}$ : at cross-section  $\sigma_{x,y} < 0.2 \, \text{mm}$  angle  $\overline{\theta} < 0.28 \, \text{mrad}$ , and at cross-section  $\sigma_{x,y} = 0.1 \, \text{mm}$  angle  $\overline{\theta}$  can be three times less than its value at experimental beam parameters

(see Fig. 3c). Increasing beam cross-section from  $\sigma_{x,y} = 0.1$  mm to values  $\sigma_{x,y} \approx 0.25$  mm measured in experiment leads to angle increase  $\overline{\theta}$ ; with further cross-section increase above experimental values and fixed emittance, no increase in angle  $\overline{\theta}$  occurs (see Fig. 3c).

The dependence  $\overline{\theta}(\sigma_e)$  on electron energy spread is shown in Fig. 3*d*. With increasing beam energy spread, there is an almost linear decrease in electron-photon interaction angle  $\overline{\theta}$ . This affects Bessel coefficients of harmonics (2) both directly and indirectly through generalized Bessel functions (3), which also depend on angular contributions  $\overline{\theta}$ . Accordingly, FEL Pierce parameters of harmonics  $\rho_n$  also depend on electron energy spread; this dependence is shown and investigated by us in Section 3.

Note also that the maximum value  $\bar{\theta}$  remains approximately the same for all beam parameter variations we studied (see Figs. 3a, b, c). Angular effects are closely related to the emission of even harmonics of undulator radiation. In relativistic beams, even harmonics of radiation arise to a lesser extent due to betatron oscillations and to a greater extent due to angular effects; the effective angle  $\bar{\theta}$  significant in FEL exceeds all other angular contributions and changes insignificantly with variation in cross-section and emittance (see Figs. 3a, c). At a given fixed emittance, the change in the angle  $\bar{\theta} \approx \sigma_{x,y}/L_{gain}$  of electronphoton interaction occurs towards smaller values with deviation of the LEUTL beam cross-section from its nominal value of  $\sigma_{x,y} \approx 0.25 \text{ mm}$  (see Figs. 3a, c). This suggests that at a given emittance in LEUTL FEL, smaller beam cross-sections may weaken even harmonics of FEL.

## 3. INFLUENCE OF ELECTRON BEAM PARAMETERS ON FEL HARMONIC RADIATION

We calculated using formulas (2)–(11) and traced the influence of electron beam parameters on Bessel coefficients and harmonic radiation powers. The effective angle of electron-photon interaction in LEUTL FEL is taken into account:  $\gamma \bar{\theta} \approx 0.14$ , which strongly affects the power of even FEL harmonics. The dependence of Bessel coefficients on beam cross-section at the fixed Twiss parameter  $\beta=1.5$  m in the experiment is graphically presented in Fig. 4a; effectively, the emittance change in this case occurs due to cross-section variation. The dependence of

Bessel coefficients on electron beam energy spread is shown in Fig. 4b for the given LEUTL beam emittance and cross-section in the experiment.

Note that the change in cross-section at fixed Twiss parameter (i.e., at given focusing) has little effect on Bessel coefficients: the value  $f_1 = 0.75$ for the fundamental tone does not change and therefore is not shown in the figures; values  $f_2$  for the second harmonic change, although slightly (see Fig. 4a), following the change in angle  $\bar{\theta}$  in Fig. 3a (orange line in Fig. 4a follows the curve in Fig. 3a). An interesting observation is the decrease in Bessel coefficients of the second harmonic  $f_2$  compared to the Bessel coefficient of the third harmonic  $f_3$ with increasing energy spread (see Fig. 4b). This allows to conclude (see Fig. 4b) that the second harmonic will apparently be more suppressed in the FEL spectrum at increased beam energy spread. At the same time, the change in cross-section (see Fig. 4a), apparently, will not have such a significant impact on the second harmonic power as the change in energy spread. For the energy spread dependence in Fig. 4b, we limited the upper range of studied values  $\sigma_e$  by the Pierce parameter  $\rho$  (5) FEL based on the condition  $\sigma_e < \rho$ . Regarding the dependence of the Bessel coefficient of the third harmonic  $f_3$  on energy spread, we note that a small increase  $f_3$  with growing electron energy spread is generally atypical and apparently related to the decrease in angular contributions in generalized Bessel functions (3) for the LEUTL FEL facility.

With real facility parameters in the LEUTL FEL experiment [40] (data provided above at the beginning of Section 2), we analytically obtained the second harmonic content in FEL radiation  $\approx 0.3\%$ , which is within the measurement spread and in good agreement with the average value measured in all experiments:  $P_2/P_1 = 1/240$  [40]. The calculated third harmonic content was  $\approx 0.8\%$ , which also agrees with the experiment; the calculated gain length  $L_g = 0.77$  m and saturation length  $L_s = 16$  m exactly correspond to the measured values [40].

Taking into account the Bessel coefficients (see Fig. 4), we analytically calculated the dependencies of the Pierce parameter  $\rho_n$  for harmonics, as well as harmonic radiation power  $P_n$  on beam cross-section and electron energy spread. The dependencies  $\rho_n$  and  $P_n$  on beam cross-section at the experimentally specified energy spread  $\sigma_e = 0.001$  are shown in Fig. 5; dependencies on energy spread at the specified

576 ZHUKOVSKY

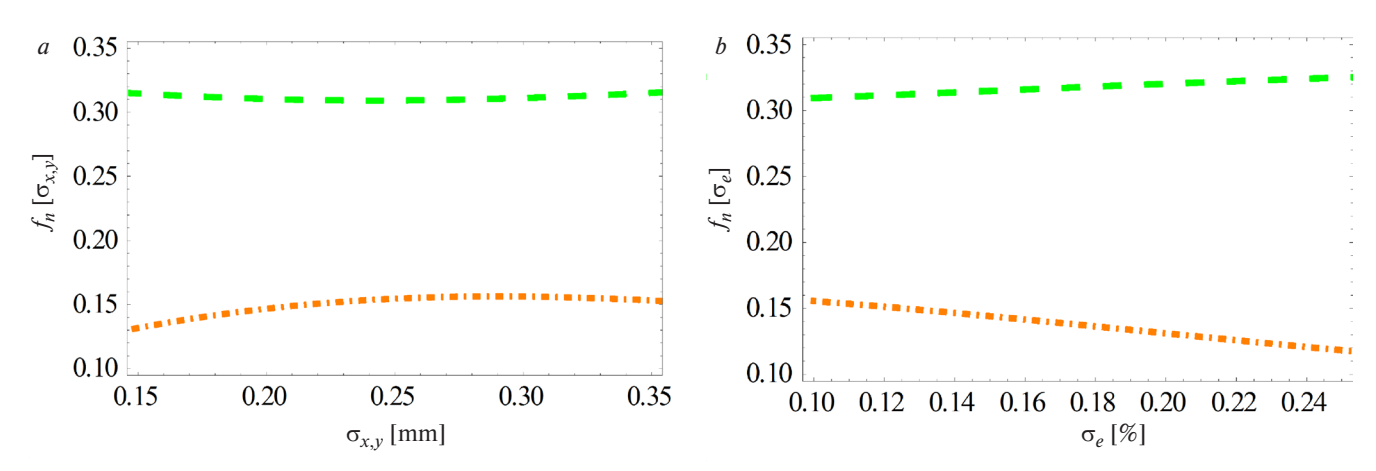


Fig. 4. Dependencies of Bessel coefficients  $f_n$  of LEUTL FEL harmonics on beam cross-section at energy spread  $\sigma_e = 0.001$  (a) and energy spread at - beam cross-section  $\sigma_{x,y} \approx 0.26$  mm (b); current  $I_0 = 210$  A, parameter  $\beta_{x,y} = 1.5$  m. Harmonics - n = 2 dash-dotted orange line, n = 3 dashed green line

cross-section  $\sigma_{x,y} \approx 0.26$  mm are shown in Fig. 6. Let's analyze in Figs. 5 and 6 the influence of beam parameters on FEL harmonic radiation.

With increasing beam cross-section  $\sigma_{x,y}$ , FEL radiation weakens due to a decrease in the Pierce parameter value, shown in Fig. 5a. As the cross-section increases, the Pierce parameter decreases (see Fig. 5a if only because increasing the beam cross-section  $\sigma_{x,y}$  reduces the electron current density in it (at fixed current I); this directly affects the Pierce parameter (5):

$$\rho_n \propto \sqrt[3]{\left(\frac{I}{\sigma_{x,y}^2}\right)} f_n |^2.$$

Generally speaking, changes in the Pierce parameter p are usually followed by changes in power; this is clearly visible in Fig. 5b. From the graphs in Fig. 5, it follows, as we assumed from the analysis of the gain length dependence on the crosssection (see Section 2), that the influence of the cross-section on radiation is approximately the same for all harmonics n = 1,2,3 (see Fig. 5). Note that the power of the second harmonic is slightly higher for cross-sections  $\sigma_{x,y} \sim 0.1-0.15$  mm and does not change when the beam cross-section increases to  $\sigma_{x,y} \approx 0.02$  mm (see orange dash-dotted line in Fig. 6a). This occurs because the second harmonic of FEL strongly depends on the effective angle  $\overline{\theta}$ , and its power follows the dependence  $\overline{\theta}$  on cross-section shown in Fig. 3a.

Changes in electron energy spread practically do not affect the Pierce parameter of odd harmonics (see Fig. 6a), but the increase in energy spread reduces the Pierce parameter  $f_{even}$  of even harmonics. This occurs mainly because  $f_{even}$  strongly depend on the angle  $\overline{\theta}$ , which decreases with increasing energy spread (see Fig. 3d). At the same time, the increase in energy spread leads to a decrease in the power of all FEL harmonics due to deterioration of electron bunching (see Fig. 6b). This is more pronounced for the second harmonic than for the third and fundamental tone, which is not related to the Pierce parameter, the corresponding change of which is shown in Fig. 6a. For energy spread in a wide range of values, the Pierce parameter of first and third harmonics practically does not change, while the Pierce parameter of the second harmonic decreases with increasing energy spread (see Fig. 6a), but not strong enough to cause the reduction in FEL second harmonic power shown in Fig. 6b. At the experimental beam cross-section of  $\sigma_{x,y} \approx 0.26$  mm, increasing the electron energy spread from 0.1% to 0.25% leads to a decrease in the fundamental tone and third harmonic radiation power by approximately three times, while the second harmonic power decreases by more than a hundred times. Comparing Fig. 5 and 6, one can see that if the Pierce parameter dependence in Fig. 5a causes power changes in Fig. 5b, then the changes in Fig. 6b are caused not only by the dependence in Fig. 6a, where the Pierce parameter  $\rho_{1,3}$  remains practically unchanged. Also, the weakening of the FEL second harmonic radiation by two orders of magnitude with an increase in energy spread from  $\sigma_e = 0.1\%$ to  $\sigma_e = 0.25\%$  (orange dash-dotted line in Fig. 6b)

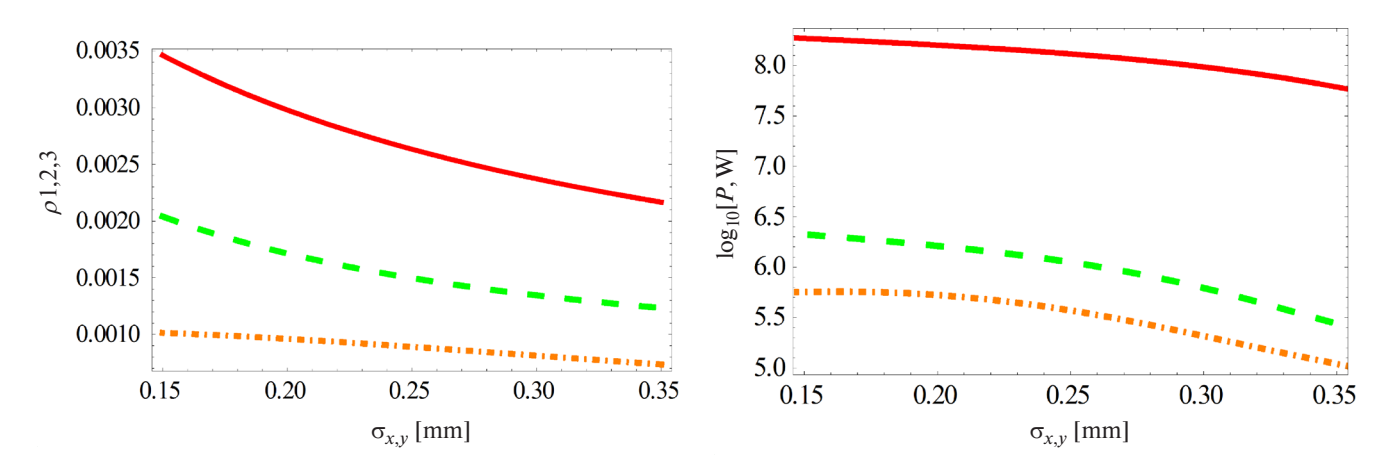
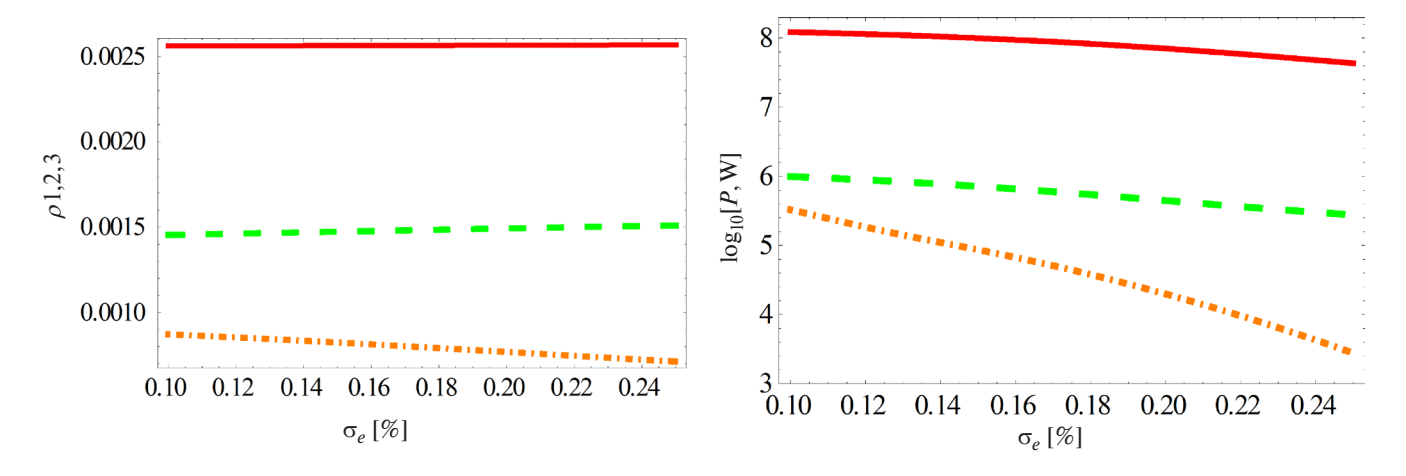


Fig. 5. Dependencies of Pierce parameter of LEUTL FEL harmonics (a) and power of LEUTL FEL harmonics (b) on beam cross-section. Energy spread  $\sigma_e = 0.001$ , current  $I_0 = 210$  A, Twiss parameter  $\beta_{x,y} = 1.5$  m; emittance changes with cross-section variation. Harmonics: n = 1 – solid red line, n = 2 – dash-dotted orange line, n = 3 – dashed green line



**Fig. 6.** Dependencies of Pierce parameter of LEUTL FEL harmonics (*a*) and power of LEUTL FEL harmonics (*b*) on energy spread. Cross-section  $\sigma_{x,y} \approx 0.26$  mm, current  $I_0 = 210$  A, Twiss parameter  $\beta_{x,y} = 1.5$  m, emittance  $\gamma \epsilon_{x,y} = 6.2\pi \cdot 10^{-6}$  mm mrad. Harmonics: n = 1 – solid red line, n = 2 – dash-dotted orange line, n = 3 – dashed green

apparently is not caused only by the change in Pierce parameter  $\rho_2$  (orange dash-dotted line in Fig. 6a).

Comparison of the influence of changes in beam cross-section and electron energy spread on the power of first and second harmonics is shown in Fig. 7; comparison of the influence on the power of first and third harmonics is shown in Fig. 8. Dependencies on beam cross-section and electron energy spread are qualitatively similar to each other, especially for first and third harmonics in Fig. 8. However, identical changes in beam parameters lead to greater changes in FEL second harmonic power than in the first (see Fig. 7). Fig. 7 shows that when beam energy spread increases twofold from  $\sigma_e \approx 0.1\%$  to  $\sigma_e \approx 0.2\%$  at given experimental values of emittance and cross-section  $\sigma_{x,y} \approx 0.26$  mm, the FEL second

harmonic power will decrease more than tenfold. If the cross-section is slightly increased from  $\sigma_{x,y} \approx 0.26$  mm to  $\sigma_{x,y} \approx 0.3$  mm, the second harmonic will be further weakened. When energy spread increases to  $\sigma_e \approx 0.25\%$  and standard beam cross-section  $\sigma_{x,y} \approx 0.26$  mm, second harmonic power will decrease approximately hundredfold, and with simultaneous increase in cross-section to  $\sigma_{x,y} \approx 0.3$  mm, we get FEL second harmonic weakening approximately two hundredfold (see Fig. 7). The fundamental tone power changes but slightly. Note that with fixed Twiss parameter  $\beta_{x,y} = 1.5$  m and cross-section increase from  $\sigma_{x,y} \approx 0.25$  mm to  $\sigma_{x,y} \approx 0.3$  mm, along with simultaneous energy spread increase from  $\sigma_e \approx 0.1\%$  to  $\sigma_e \approx 0.2\%$ , FEL power will decrease approximately threefold, second harmonic

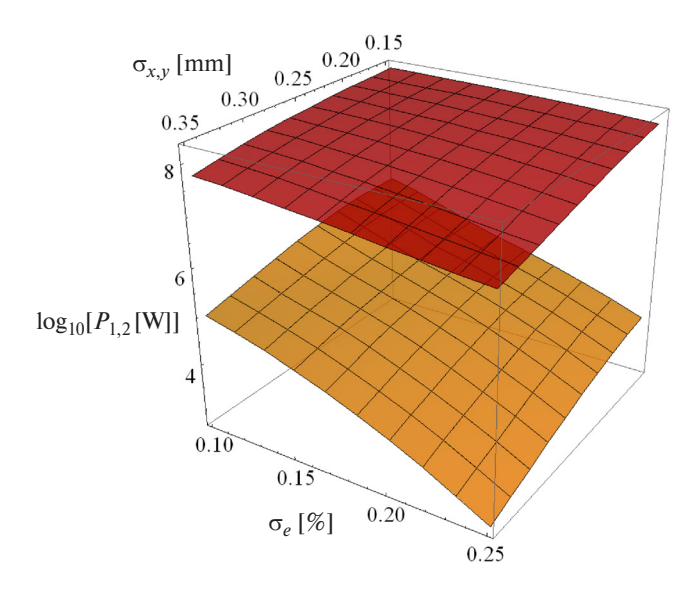


**Fig. 7.** Dependence of power of first and second LEUTL FEL harmonics on energy spread and electron beam cross-section at current  $I_0 = 210$  A; Twiss parameter  $\beta_{x,y} = 1.5$  m

power — by more than an order of magnitude (see Fig. 7), and gain length will increase from  $c \approx 0.77$  m to  $c \approx 1.33$  m (see Fig. 1a). The same FEL power decrease is expected with unchanged cross-section  $\sigma_{x,y} \approx 0.26$  mm and 2.5 times increased energy spread  $\sigma_e \approx 0.25\%$ . In this case, gain length grows somewhat slower (see Fig. 1a) and reaches 1.2 m.

Thus, using increased electron energy spread with unchanged beam cross-section, we gain advantage in shorter gain length with the same FEL power decrease as in the case of increased cross-section with unchanged energy spread.

Note that the behavior of the FEL third harmonic when changing parameters is very similar to the behavior of the fundamental tone (compare green n = 3 and red n = 1 surfaces in Fig. 8). The content of the second harmonic in the LEUTL FEL radiation depending on the cross-section and energy spread of the beam is shown in Fig. 9. Note that changing the cross-section barely affects the second harmonic content, while increasing energy spread significantly reduces the second harmonic content. Thus, to suppress the FEL second harmonic, it is better to increase the energy spread rather than the beam cross-section or emittance. The dependence of the FEL radiation second harmonic content on energy spread is close to exponential with a negative exponent: in Fig. 9 on a logarithmic scale, the decrease  $\log_{10}(P_2/P_1)$  with increase  $\sigma_{\rho}$  occurs almost linearly.

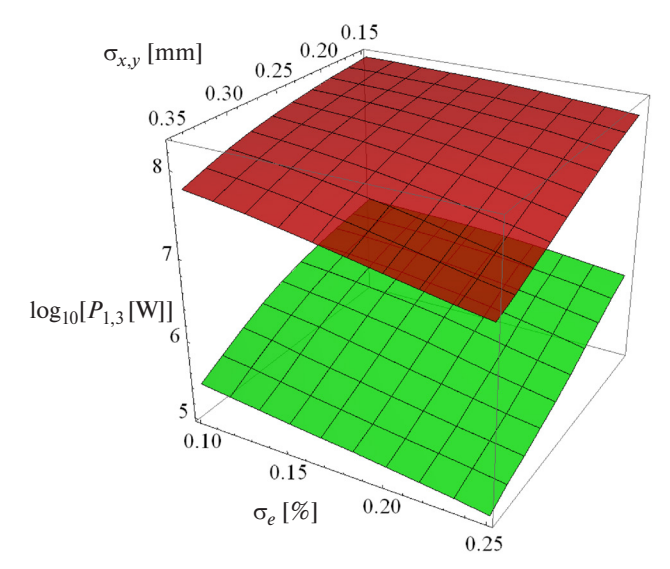


**Fig. 8.** Dependence of power of first and third harmonics of LEUTL FEL on energy spread and electron beam cross-section at current  $I_0 = 210$  A; Twiss parameter  $\beta_{x,y} = 1.5$  m

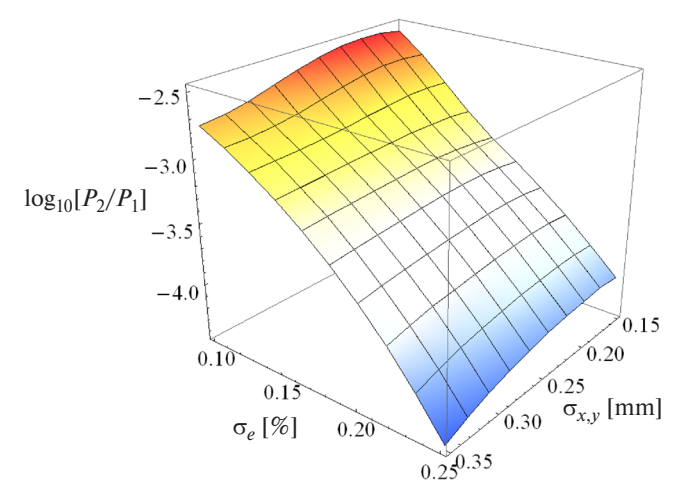


**Fig. 9.** Dependence of second harmonic content in LEUTL FEL radiation on electron energy spread and beam cross-section at current  $I_0 = 210$  A; Twiss parameter  $\beta_{x,y} = 1.5$  m

In conclusion, let's compare the influence of increased electron energy spread with the effect of the undulator field second harmonic on FEL second harmonic radiation, recently studied in [57, 58]. These works demonstrated the possibility to reduce the FEL second harmonic using the undulator magnetic field second harmonic in antiphase with the main field. According to the results in [57, 58], the second field harmonic

$$H_{2,d} = H_0 d \sin(4\pi z/\lambda_u)$$

with relative amplitude  $d \approx -0.1$  of the main undulator field

$$H = H_0 \sin(2\pi z/\lambda_u)$$

allows reducing FEL second harmonic radiation by approximately an order of magnitude (the degree of field harmonic influence depends on installation parameters). Electron bunching occurs in the field of two waves excited at different undulator harmonics. If the waves or their harmonics arrive in phase, then bunching at this wavelength becomes stronger, and if in antiphase, then weaker. A similar two-frequency effect occurs in millimeter-range cyclotron amplifiers. Usually, efforts are made to improve electron bunch grouping; for example, in [59–61] it was shown that in cyclotron masers, using particle bunching in the field of two waves excited at the first and second cyclotron harmonics provides substantial improvement in electron bunching. The influence of energy spread was not considered in this case. Similarly, by varying the amplitude and phase of the field harmonic in undulators, one can change the content of the corresponding harmonic in radiation while barely affecting the fundamental tone power (see [42, 44, 45, 62] and others).

We compared and analyzed the combined effect of the second harmonic of the undulator field and electron beam spread  $\sigma_e$  on the FEL radiation power. Applying formulas (5)–(11) for analytical calculation of FEL harmonic power, we used Bessel coefficients for a two-frequency undulator taking into account the second field harmonic from [58]:

$$f_{n;x} \approx \sum_{p} \tilde{J}_{p} | (J_{n+1}^{n} + J_{n-1}^{n}) + \frac{d}{h} (J_{n+h}^{n} + J_{n-h}^{n}) + J_{n}^{n} \frac{2}{k} \gamma \theta \cos \varphi |,$$

$$f_{n;y} \approx \sum_{p} (\tilde{J}_{p} | J_{n}^{n} \frac{2}{k} \gamma \theta \sin \varphi | + \frac{1}{n} \frac{\sqrt{2} \pi y_{0}}{\lambda_{u}} ((\tilde{J}_{p+1} - \tilde{J}_{p-1}) + \frac{d}{h} (\tilde{J}_{p+h} - \tilde{J}_{p-h}))),$$
(13)

where d is the amplitude of the undulator field harmonic with number h; in particular, in our case of interest h = 2. Bessel coefficients (13) have more complex form than (2) and account for the field

harmonic influence explicitly in (13) and implicitly in the following arguments:

$$\xi_{0} = \frac{2d\gamma\theta\cos\phi\sin(h\alpha)}{kh^{2}}, \qquad \xi_{1} = \frac{\sin(2\alpha)}{4},$$

$$\xi_{2} = \frac{d\sin((h-1)\alpha)}{h(h-1)}, \qquad \xi_{3} = \frac{d\sin((h+1)\alpha)}{h(h+1)},$$

$$\xi_{4} = \frac{d^{2}\sin(2h\alpha)}{4h^{3}}, \qquad \xi_{5} = \frac{2}{k}\gamma\theta\cos\phi\sin\alpha, \qquad (14)$$

$$\kappa = \frac{4\pi\theta y_{0}\gamma^{2}}{\lambda_{u}(1+k^{2}/2)}, \qquad \eta = \frac{\pi^{2}\gamma y_{0}^{2}k}{\sqrt{2}\lambda_{u}^{2}(1+k^{2}/2)},$$

in generalized Bessel functions

$$J_{n}^{m} = \int_{-\pi}^{\pi} \frac{d\alpha}{2\pi} \times \exp\left\{i\left(n\alpha + \frac{mk^{2}(\xi_{0} + \xi_{1} + \xi_{2} + \xi_{3} + \xi_{4} + \xi_{5})}{1 + \gamma^{2}\theta^{2} + k_{eff}^{2}/2}\right)\right\}, \quad (15)$$

$$\tilde{J}_{p} = \int_{-\pi}^{\pi} \frac{d\alpha}{2\pi} \exp\left\{i\left(p\alpha - \kappa\sin\alpha - \eta\sin(2\alpha)\right)\right\}.$$

As a result, in addition to the previously obtained dependence of gain length and harmonic power on beam cross-section, emittance, and energy spread, we obtained their dependencies on the amplitude  $H_{h=2,d} = H_0 d$  of the second harmonic of the undulator field. The dependence of Bessel coefficients on the second field harmonic in the undulator is shown in Fig. 10a. The negative phase of the second field harmonic decreases the Bessel coefficient  $f_2$ of the second FEL harmonic and thus reduces its radiation power in the FEL. The positive phase of the second field harmonic increases the Bessel coefficient  $f_2$  (orange dash-dotted line in Fig. 10a) and decreases the Bessel coefficient of the third harmonic  $f_3$  (green dashed line in Fig. 10a). This leads to corresponding changes in the power of these harmonics in radiation, as shown in Fig. 10b. The Bessel coefficient of the fundamental  $f_1$  (red solid line in Fig. 10a) does not change under the influence of the second harmonic of the undulator field; the FEL power also remains unchanged (red solid line in Fig. 10b), while the radiation powers of harmonics change, following the change in  $f_{2,3}$ .

Thus, by varying the amplitude of the second field harmonic d, one can change the content of the second radiation harmonic without changing the FEL

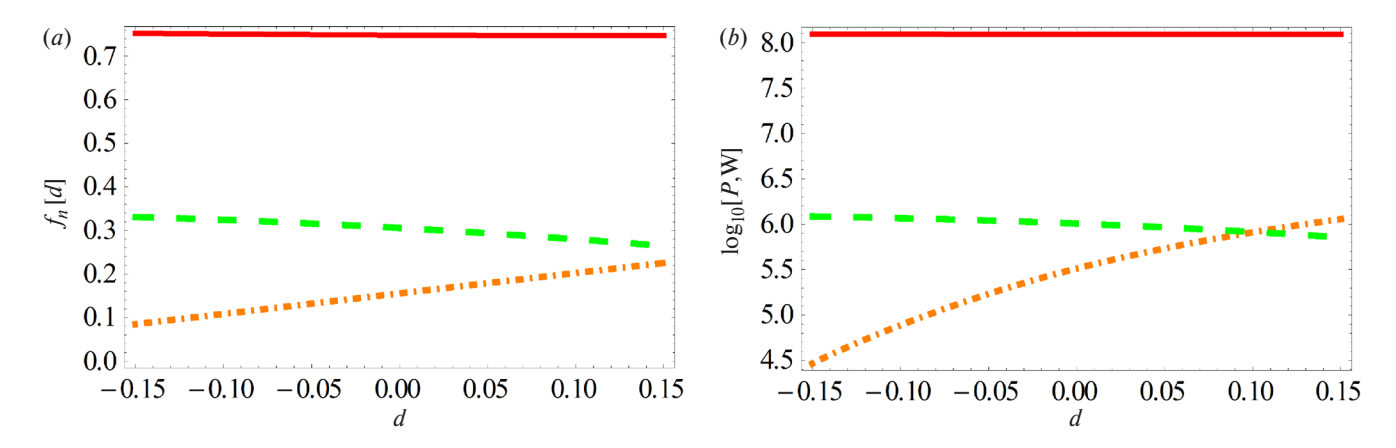


Fig. 10. Dependencies of Bessel coefficients  $f_n(a)$  and radiation power of harmonics (b) of LEUTL FEL on the relative amplitude of the second harmonic of the undulator field d at  $I_0 = 210$  A,  $\sigma_{x,y} \approx 0.26$  mm,  $\beta_{x,y} = 1.5$  m and  $\sigma_e = 0.001$ . Radiation harmonics: n = 2 – dash-dotted orange line, n = 3 – dashed green line

power itself; the content of the third harmonic in the FEL spectrum changes little when the amplitude of the second field harmonic changes (see Fig. 10*b*).

The combined influence of the second harmonic of the undulator field and the beam energy spread on the content of the second harmonic in the LEUTL FEL radiation spectrum is shown in Fig. 11.

Note that the increase in electron energy spread and the amplitude of the second harmonic of the undulator field in antiphase to the main field mutually enhance the suppression of FEL second harmonic radiation (see Fig. 11). With energy spread  $\sigma_e = 0.001$ we have a relatively weak dependence of the d second harmonic radiation power on the amplitude of the second harmonic of the undulator field: at d = -0.1there is a decrease in FEL second harmonic content by 5–7 times [58], and at d = 0 we have the results presented above in this work. In the remaining part of Fig. 11, we see that the second harmonic of the undulator field and electron energy spread effectively "help" each other in suppressing FEL second harmonic radiation: at  $\sigma_{\rho} = 0.0025$ , the second harmonic of the field with a relative amplitude d = -0.1 weakens the radiation of the second harmonic of the FEL by two orders of magnitude of power (see Fig. 11). Note that in the LEUTL experiments with a standard undulator and an energy spread of  $\sigma_e = 0.001$ , the content of the second harmonic of the FEL was about 0.1-0.5%; in Fig. 11 this corresponds to the far angle, where

$$\log_{10} \frac{P_2}{P_1} \Big|_{d=0,\sigma_e=0.001} \approx -2.5.$$

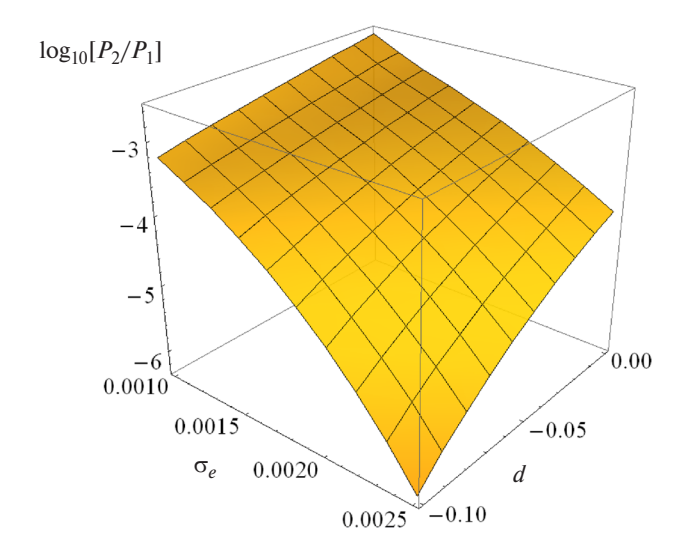


**Fig. 11.** Dependence of the second harmonic content in LEUTL FEL radiation on electron energy spread and amplitude of the second harmonic of the undulator field at the following parameter values:  $I_0 = 210$  A,  $\beta_{x,y} = 1.5$  m,  $\sigma_{x,y} = 0.26$  mm,  $\gamma \varepsilon_{x,y} = 6.2\pi \cdot 10^{-6}$  mm·mrad

By doubling the energy spread to  $\sigma_e = 0.002$  and adding to the undulator field in antiphase the second harmonic with amplitude 5% of the main field, d = -0.05, we get the FEL second harmonic content two orders of magnitude lower:

$$\log_{10} \frac{P_2}{P_1} \bigg|_{d=-0.05, \sigma_{\rho}=0.002} \approx -4.5.$$

With the second harmonic field amplitude d = -0.1 and with 2.5 times increased energy spread  $\sigma_e = 0.002$  we get even lower second harmonic content in FEL radiation:

$$\log_{10} \frac{P_2}{P_1} \bigg|_{d=-0.1,\sigma_e=0.0025} \approx -6.$$

Thus, increasing the electron energy spread can significantly weaken the second harmonic radiation, but increases the FEL gain length. The second harmonic of the undulator field with reverse phase also weakens the FEL second harmonic radiation while not affecting the FEL gain length and fundamental tone power, which allows maintaining the FEL size without serious cost increase. The influence of the second harmonic field is somewhat more effective at large beam energy spreads.

Additional velocity spread of electrons can apparently be arranged already at the stage of bunch formation in the photoinjector. There, electron energies are small, and the spread is acquired, for example, due to the Coulomb fields of the bunch or due to time irregularities in the accelerating field (when different electrons are accelerated by different fields).

### 4. CONCLUSIONS

A theoretical analysis of the electron beam parameters' influence on FEL radiation and harmonic generation has been conducted. An example of the well-documented LEUTL FEL with radiation in the visible range at a wavelength of  $\lambda_1\approx 540\,$  nm is considered. The formalism of generalized Bessel functions was used, where the main FEL parameters are analytically accounted for. The simulation results of LEUTL FEL harmonic powers fully agree with experimental data. Analysis of the influence of beam cross-section, emittance, and energy spread on the gain length and FEL radiation harmonic powers was performed.

It is analytically shown how increasing energy spread, cross-section, and beam emittance increases the gain length and decreases FEL radiation harmonic powers. In the case of fixed Twiss parameter, cross-section increase occurs due to emittance increase; this leads to a more significant growth in FEL gain length compared to the case of fixed emittance and cross-section change due to Twiss parameter variation  $\beta$ .

Approximately equal influence of beam crosssection increase and electron energy spread on the first and third harmonic powers of LEUTL FEL radiation has been demonstrated.

It is shown how beam cross-section variation and the resulting change in FEL gain length alter the electron-photon interaction angle. The angle change is  $\overline{\theta}$  greater with fixed emittance than with fixed Twiss parameter for the same cross-section variation. Angular effects associated with  $\overline{\theta}$ , in turn, determine the generation of even FEL harmonics.

It is analytically shown that increasing electron energy spread increases FEL gain length and weakens the generation of all radiation harmonics; even harmonics are particularly strongly suppressed (compare with Figs. 7 and 8). Beam cross-section variation has less influence on second harmonic power than electron energy spread variation. Thus, suppression of FEL second harmonic requires an increase in energy spread rather than beam cross-section or emittance.

Analysis of harmonic powers of LEUTL FEL depending on energy spread  $\sigma_e$  and beam cross-section  $\sigma_{x,y}$  leads to the following estimation: regardless of the beam cross-section, the change in the second harmonic radiation content follows a law close to exponential with a negative exponent:

$$\log_{10}\frac{P_2}{P_1}\sim -\sigma_e,$$

see Fig. 1.

It is shown that it is possible to reduce the second harmonic content of LEUTL FEL by an order of magnitude by increasing the beam energy spread twofold from 0.1% to 0.2%. Moreover, increasing the energy spread from 0.1% to 0.25% reduces the second harmonic content of FEL by almost two orders of magnitude. In this case, the total FEL power decreases several times and the gain length doubles. This method of reducing the FEL second harmonic content appears to be the simplest and is feasible, for example, by increasing the electron energy spread already in the photoinjector.

Reduction of FEL second harmonic power is possible using the second harmonic of the undulator field in antiphase to the main field. It is shown that the effects of the undulator field second harmonic and increased electron energy spread mutually reinforce each other and effectively suppress the FEL second harmonic radiation. A twofold increase in electron energy spread from  $\sigma_e = 0.1\%$  to  $\sigma_e = 0.2\%$  and simultaneous use of an undulator with a second field harmonic with amplitude 5% of the main field reduces the FEL second harmonic content by two orders of magnitude. Increasing the energy spread to  $\sigma_e = 0.25\%$  and the second field harmonic with

amplitude 10% of the main field further reduces the FEL second harmonic content to  $P_2/P_1 \sim 0.0001\%$ .

Using a dual-frequency undulator with field harmonic is technically difficult to implement, but it allows changing the second harmonic content in the spectrum without changing the total radiation power and without changing the FEL gain length.

The obtained results can be used in theoretical and applied research and experiment design when analyzing the nonlinear response of second harmonic generation (SHG) with a coherent FEL radiation source.

### **ACKNOWLEDGMENTS**

The author thanks I. Papp for formatting the article in LaTeX format.

### **FUNDING**

This work was supported by the Ministry of Education and Science of Russia (grant No. 075-15-2021-1353).

#### REFERENCES

- 1. V.L. Ginzburg, Izv. AN SSSR (Physics) 11, 165 (1947).
- H. Motz, W. Thon, and R.N.J. Whitehurst, Appl. Phys. 24, 826 (1953).
- 3. J.M. Madey, J. Appl. Phys. 42, 1906 (1971).
- **4.** *G. Margaritondo*, Rivista del Nuovo Cimento **40**, 411 (2017).
- V.G. Bagrov, G.S. Bisnovatyi-Kogan, V.A. Bordovitsyn et al., Theory of Radiation of Relativistic Particles, Fizmatlit, Moscow (2002).
- **6.** I.M. Ternov, V.V. Mikhailin, V.R. Khalilov, Synchrotron Radiation and Its Applications, Moscow State University Publishing House, Moscow (1980).
- G. Margaritondo, Characteristics and Properties of Synchrotron Radiation, in Synchrotron Radiation, ed. by S. Mobilio, F. Boscherini, and C. Meneghini, Springer, Berlin, Heidelberg (2015).
- **8.** B.W.J. McNeil and N.R. Thompson, Nature Photonics **4**, 814 (2010).
- **9.** *C. Pellegrini, A. Marinelli, and S. Reiche*, Rev. Mod. Phys. **88**, 015006 (2016).
- P. Schmuser, M. Dohlus, J. Rossbach, and C. Behrens, Free-Electron Lasers in the Ultraviolet and XRay Regime, Springer Tracts Mod. Phys., 258, Cham (ZG): Springer Int. Publ. (2014).
- **11.** *Z. Huang and K.J. Kim*, Phys. Rev. ST Accel. Beams **10**, 034801 (2007).

- **12.** *G. Margaritondo and P.R. Ribic*, J. Synchrotron Rad. **18**, 101 (2011).
- **13.** E.L. Saldin, E.A. Schneidmiller, and M.V. Yurkov, The *Physics of Free Electron Lasers*, Springer-Verlag, Berlin, Heidelberg (2000).
- **14.** *R. Bonifacio, C. Pellegrini, and L. Narducci*, Opt. Comm. **50**, 373 (1984).
- **15.** *T. Sumi, M. Horio, T. Senoo et al.*, E-J. Surf. Sci. Nanotech. **20**, 31 (2021), DOI: 10.1380/ejssnt.2022–002.
- **16.** *S. Shwartz, M. Fuchs, J.B. Hastings et al.*, Phys. Rev. Lett. **112**, 163901 (2014).
- **17.** *S. Yamamoto, T. Omi, H. Akai et al.*, Phys. Rev. Lett. **120**, 223902 (2018).
- 18. E. Berger, S. Jamnuch, C. Uzundal et al., arXiv: 2010.03134.
- **19.** *R.K. Lam, S.L. Raj, T.A. Pascal et al.*, Phys. Rev. Lett. **120**, 023901 (2018).
- **20.** *L.Wu, S. Patankar, T. Morimoto et al.*, Nature Phys. **13**, 350 (2016).
- **21.** *M. Nuriya, S. Fukushima et al.*, Nature Commun. **7**, 11557 (2016).
- **22.** C.P. Schwartz, S.L. Raj, S. Jamnuch et al., arXiv: 2005.01905.
- **23.** *P.J. Campagnola and L.M. Loew*, Nature Biotechnol. **21**, 1356 (2003).
- **24.** *T. Helk, E. Berger, S. Jamnuch et al.*, Sci. Adv. 7, 2265 (2021).
- 25. G. Boyd, T. Bridges, and E. Burkhardt, IEEE J. Quant. Electron. 4, 515 (1968).
- **26.** *G.C. Bhar, S. Das, and K.L. Vodopyanov*, Appl. Phys. B **61**, 187 (1995).
- 27. K. Zhukovsky, Opt. Laser Technol. 131, 106311 (2020).
- 28. K. Zhukovsky, Eur. Phys. J. Plus 136, 714 (2021).
- 29. K. Zhukovsky, Ann. Phys. 533, 2100091 (2021).
- 30. K. Zhukovsky, Rad. Phys. Chem. 189, 109698 (2021).
- **31.** *K. Zhukovsky*, Opt. Laser Technol. **143**, 107296 (2021).
- 32. K. Zhukovsky, Results Phys. 19, 103361 (2020).
- **33.** *K. Zhukovsky and I. Fedorov*, Symmetry **13**, 135 (2021).
- **34.** *J.R. Henderson, L.T. Campbell, H.P. Freund, and B.W.J. McNeil*, New J. Phys. **18**, 062003 (2016).
- **35.** *H.P. Freund, P.J. M. van der Slot, D.L.A.G. Grimminck et al.*, New J. Phys. **19**, 023020 (2017).
- **36.** *H.P. Freund and P.J.M. van der Slot*, New J. Phys. **20**, 073017 (2018).
- **37.** *P. Emma, R. Akre, J. Arthur et al.*, Nature Photonics **4**, 641 (2010).
- **38.** *D. Ratner, A. Brachmann, F.J. Decker et al.*, Phys. Rev. ST Accel. Beams **14**, 060701 (2011).
- **39.** *S.V. Milton, E. Gluskin, N.D. Arnold et al.*, Science **292**, 2037 (2001).
- **40.** *S.G. Biedron et al.*, Nucl. Instrum. Meth. A **483**, 94 (2002).

- **41.** *L. Giannessi et al.*, Phys. Rev. ST Accel. Beams **14**, 060712 (2011).
- 42. K.V. Zhukovsky, Russ. Phys. J. 62 (6), 1043 (2019).
- **43.** *H.P. Freund and P.J.M. van der Slot*, J. Phys. Commun. **5**, 085011 (2021).
- 44. K. Zhukovsky and A. Kalitenko, J. Synchrotron Rad. 26, 159 (2019).
- **45.** *K.V. Zhukovsky and A.M. Kalitenko*, Russ. Phys. J. **62 (2)**, 354 (2019).
- **46.** K.V. Zhukovsky, Physics-Uspekhi **64**, 304 (2021).
- **47.** B. Prakash, V. Huse, M. Gehlot, and G. Mishra, Optik **127**, 1639 (2016).
- **48.** *V.L. Bratman, N.S. Ginzburg, and M.I. Petelin*, Opt. Comm. **30**, 409 (1979).
- 49. M. Xie, Nucl. Instrum. Meth. A 445, 59 (2000).
- **50.** *M. Xie*, Proc. 1995 *Particle Accelerator Conf.*, IEEE, Piscataway, NJ, **183** (1995).
- G. Dattoli, P.L. Ottaviani, and S. Pagnutti, J. Appl. Phys. 97, 113102 (2005).
- **52.** G. Dattoli, L. Giannessi, P.L. Ottaviani, and C. Ronsivalle, J. Appl. Phys. **95**, 3206 (2004).
- 53. L. Giannessi, Seeding and Harmonic Generation in Free-Electron Lasers, Synchrotron Light Sources and Free-Electron Lasers, ed. by E.J. Jaeschke et al.,

- Switzerland, Springer Int. Publ. (2016), DOI: 10.1007/978-3-319-14394-1 3.
- **54.** *Z. Huang and K.-J. Kim*, Nucl. Instrum. Meth. A **475**, 112 (2001).
- **55.** *G. Geloni, E. Saldin, E. Schneidmiller, and M. Yurkov*, Opt. Comm. **271**, 207 (2007).
- **56.** *K. Zhukovsky, I. Fedorov, and N. Gubina*, Opt. Laser Technol. **159**, 108972 (2023).
- 57. K. Zhukovsky, Europhys. Lett. 141, 45002 (2023).
- **58.** *K.V. Zhukovsky*, JETP **164**, 315 (2023) [K.V. Zhukovsky, JETP **137**, 271 (2023)].
- **59.** *A.V. Savilov and G.S. Nusinovich*, Phys. Plasmas **14**, 053113 (2007).
- 60. D.D. Krygina, N.Y. Peskov, and A.V. Savilov, Frequency Multiplication in a Powerful Terahertz FreeElectron Maser, 2021 46th Int. Conf. on Infrared, Millimeter, and Terahertz Waves (IRMMW-THz), Chengdu, China (2021), DOI: 10.1109/IRMMWTHz50926.2021.9567533.
- **61.** *A.V. Savilov and G.S. Nusinovich*, Phys. Plasmas **15**, 013112 (2008).
- **62.** *A.M. Kalitenko and K.V. Zhukovsky*, JETP **157**, 394 (2020) [A.M. Kalitenko and K. V. Zhukovskii, JETP **130**, 327 (2020)].